

Method for the calculation of excitonic effects in the absorption spectra of some metals

D. J. Groh*

Department of Physics, University of Illinois at Urbana-Champaign, 1110 West Green Street, Urbana, Illinois 61801

A. B. Kunz

College of Engineering, Michigan Technological University, Houghton, Michigan 49931

C. R. Givens

Department of Mathematics, Michigan Technological University, Houghton, Michigan 49931

(Received 17 July 1989; revised manuscript received 19 December 1989)

Due to the long-range screening behavior of electrons in metals, interactions between excited electrons and their corresponding holes are weak and are generally ignored. In this paper, we attempt to include this electron-hole interaction into the calculation by randomly choosing a finite number of electron-hole states to represent the excitations and calculating the response of these chosen electrons to the excited electron. In doing so, the Coulomb interactions are scaled to compensate for the finite sample chosen. Calculations were done for lithium, sodium, potassium, calcium, and aluminum.

I. INTRODUCTION

A. Absorption spectra of metals

The absorption spectra of all metals have two main contributions. The first contribution, called the Drude absorption, has the form $\mu(E_\gamma) = 4\pi\alpha n / [m_{\text{op}}\zeta(E_\gamma)E_\gamma^2]$, where μ is the absorption coefficient, E_γ is the photon energy, α is the fine-structure constant ($\approx \frac{1}{137}$), n is the valence-electron number density, m_{op} is the optical effective mass, and $\tau(E_\gamma)$ is the frequency-dependent relaxation time.¹ τ is an approximately constant function of E for most metals² and is between 300 and 1500 for the metals of interest at room temperature. (The atomic system of units is used, in which $e^2 = \hbar = m = 1$.)

m_{op} can be measured from the real part of the dielectric function, $\text{Re}\epsilon = 1 - 4\pi n / m_{\text{op}} / E_\gamma^2$, and is generally between 1 and 2. Or, m_{op} can be calculated theoretically from the band structure

$$m_{\text{op}} = 3[(2\pi)^3/v] \left[\int d\mathbf{k} \nabla_{\mathbf{k}}^2 E(\mathbf{k}) \right]^{-1},$$

where v is the volume of the unit cell, $E(\mathbf{k})$ is the energy of the valence band at \mathbf{k} , and the integration is over the Brillouin zone.³

The second contribution to the absorption spectra is the direct interband absorption spectrum. It has the theoretical value

$$\mu(E_\gamma) = (4/3\pi)^2 / (\alpha/E_\gamma) \langle |\nabla_{F_I}| \rangle g_J(E_\gamma),$$

where $\langle |\nabla_{F_I}| \rangle$ is the average optical matrix element between all final states $|F\rangle$ and all initial states $|I\rangle$ with the same energy difference $E_I - E_F = E_\gamma$ and $g_J(E_\gamma)$ is the joint density of states at E .⁴ (Of course, for direct optical absorption, $|F\rangle$ and $|I\rangle$ must have the same net spin and the same net wave vector.)

Phonon-induced indirect transitions do play a role in the absorption spectrum but are not considered here. Generally, indirect transitions tend to broaden the spectrum (especially threshold edges and any threshold-edge singularities in the spectrum).²

B. Excitonic effects

Usually the initial states $|I\rangle$ and the final states $|F\rangle$ are assumed to be adequately described by independent-electron (uncorrelated) bands.⁸ But this is definitely not the case for all metals. Threshold singularities (called excitons) have been found experimentally in many metals in the x-ray region. These singularities cannot be calculated using any standard independent-electron theory and must be calculated by some many-electron theory. The method described here is an internally consistent way of describing simultaneously the shape and size of these excitonic features.

Excitons have been known to exist in semiconductors but due to metallic screening the electron-hole interaction in metals is weak and short range compared to the electron-hole interaction in semiconductors. Due to screening, excitonic bound states are not believed to occur in metals,⁵ but excitonic edge singularities (not quite bound states) are known to exist, and it is these singularities that are the topic of this paper.

Boisvert *et al.*⁶ and Woodward⁷ have performed finite-size cluster calculations for elemental metals and alloys. These calculations show the existence of a bound localized excited state, an exciton, with energies just below threshold (for the metals Mg, Na, and K). These local excited states are believed to have high optical absorption—thus implying peaks at the thresholds of the appropriate x-ray spectra. But these cluster calculations are incomplete since they only yield the localized excited

state which stays within the cluster and is not heavily screened.

Mahan⁸ calculated the shape of the x-ray edges to be

$$\mu(E_\gamma) = [E_0 / (E_\gamma - E_t)]^{\alpha_1} f(E_\gamma) \Theta(E_\gamma - E_t)$$

where E_0 is a typical bandwidth energy of magnitude e_F , the Fermi energy; E_t is the threshold energy; $f(E_\gamma)$ is a slowly varying function of E_γ ; and $\Theta(E_\gamma - E_t)$ is the step function. Nozières and De Dominicis⁹ derived α_1 :

$$\alpha_1 = (2\delta_2/\pi) - \sum_{l'=0}^{\infty} (2l'+1)(2\delta_{l'}/\pi)^2,$$

where l is the angular momentum of the valence state and the δ_l are phase shifts calculated from the scattering of the valence states by the electron-hole potential. So far, calculations for the δ_l have yielded too high results which must be scaled down to fit sum rules. The scaled-down results for the δ_l yield the correct signs for the α_1 , but the actual values are only moderately accurate.¹⁰⁻¹⁴ The α_1 are normally obtained directly by fitting them to the experimental data; the fitted α_1 give acceptable results for the shape of the edge. Mahan's result is incomplete since it only states the shape of the edge in terms of unknown or only approximately known parameters. The results of this paper are consistent with Mahan's results, but represent an improvement in that the results of this work have only one unknown parameter E_t , the threshold energy (which can be found for most metals in Ref. 15), versus three unknown parameters in Mahan's theory.

More general theories of many-electron effects on x-ray spectra can be found in Refs. 16 and 17. Kunz and Flynn¹⁸ have proposed that since an electron-hole pair is not an exact eigenvalue of the many-electron Hamiltonian, it interacts with other electron-hole pairs of the same total \mathbf{k} vector through the nonaverage parts of the Coulomb interaction. Thus, if one allows the excited states to include Slater determinants containing other electron-hole pairs (again, all such determinants must have the same wave vector), a much better understanding of the excitonic effects in metals can be obtained.

Results by Kunz and Flynn¹⁹ for magnesium have shown much improved results (over all previous independent-electron results) and have shown the possible existence of an excitonic resonant state in the magnesium spectrum above the absorption edge. (See Fig. 1.)

Excitonic threshold singularities have been experimentally found at the $2p$ - $3s$ transition in sodium,²⁰ the $3p$ - $4s$ transition in potassium,²¹ the $4p$ - $5s$ transition in rubidium,²¹ the $5p$ - $6s$ transition in cesium,²¹ and the $2p$ - $3s$ (Ref. 22) and $3s$ - $3p$ (Ref. 23) transition thresholds in magnesium. In addition to these, we believe that excitonic thresholds exist at all the p - s transitions in all the alkalis and the $2s$ - $2p$ transition threshold in beryllium.

A possible excitonic peak exists in the $4s$ - $4p$ transition in calcium,²⁴ but our results are consistent with this being a nonexcitonic peak due to a large density of p states only at the very edge of the interband threshold.

This research project deals with these excitonic threshold effects in certain metals, particularly those metals with convenient crystal structures, with known band

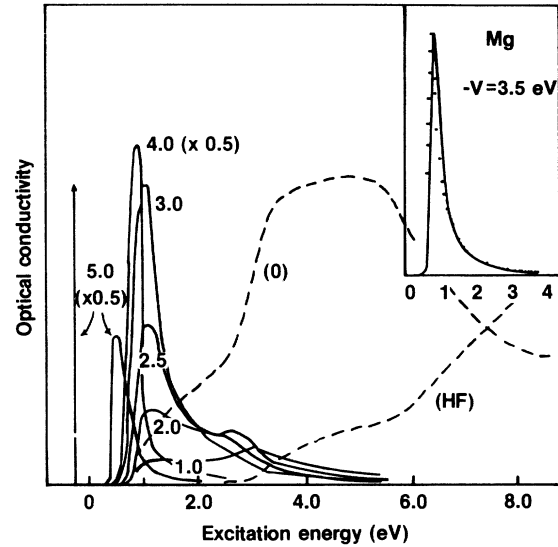


FIG. 1. Results by Kunz and Flynn (Ref. 18) for the correlated optical absorption spectra of magnesium for various values of the electron-hole interaction (stated in the text as $\langle u', v' | H | u, v \rangle$). In the upper right of the graph is a comparison of the experimental results (dots) with the theoretical values (solid curve) using an electron-hole interaction value of -3.5 eV (which is an overestimate; -2.1 eV is a more reasonable value but -3.5 eV gives a better comparison with experiment).

structures, and with electron states that can be described with only a few angular momentum states.

II. THEORY

A. Wave function

Electronic wave functions must be linear combinations of Slater determinants, determinants of the independent-electron wave functions.²⁵ Ψ^I will denote the wave function I ; ψ_A will denote the A th Slater determinant; and Φ_i will denote the i th independent-electron wave function, which includes a spinor. Since the systems dealt with are crystalline, these may be Bloch sums of local orbitals,

$$\Phi_i(\mathbf{r}) = N_L^{-1/2} \sum_{\mathbf{R}} \exp(i\mathbf{k}_i \cdot \mathbf{R}) \phi_i(\mathbf{r} - \mathbf{R}),$$

$$\Psi^I = \sum_A \alpha_A^I \psi_A,$$

$$\psi = /N!^{-1/2} \begin{vmatrix} \Phi_{A_1}(\mathbf{r}_1) & \Phi_{A_1}(\mathbf{r}_2) & \cdots & \Phi_{A_1}(\mathbf{r}_N) \\ \Phi_{A_2}(\mathbf{r}_1) & \Phi_{A_2}(\mathbf{r}_2) & \cdots & \Phi_{A_2}(\mathbf{r}_N) \\ \vdots & \vdots & \ddots & \vdots \\ \Phi_{A_N}(\mathbf{r}_1) & \Phi_{A_N}(\mathbf{r}_2) & \cdots & \Phi_{A_N}(\mathbf{r}_N) \end{vmatrix},$$

where N is the number of electrons, or in second quantization notation,

$$|\psi_A\rangle = a_{A_1}^\dagger a_{A_2}^\dagger \cdots a_{A_N}^\dagger |0\rangle$$

where the creation operator, a_k^\dagger , occupies the state Φ_k .

(Conversely, the annihilation operator a_k deoccupies the state Φ_k .) The ground state will have $A_1=1$, $A_2=2$, . . . , $A_N=N$. And the excited state will have some of the A_i not between 1 and N and an equal amount of the A_i greater than N .

B. Simplified LCAO

The ϕ_i are determined from a fitting method developed by Slater and Koster²⁶ called simplified linear combination of atomic orbitals (LCAO). This method involves

fitting energy integrals to published band structures. The band structures used are listed in Ref. 27.

One starts with a basis set of one arbitrary, unknown radial wave function for each angular momentum type used (up to some maximum angular momentum l_{\max} , set to 2 for this project), i.e.,

$$\phi_i(\mathbf{r}) = \sum_{l=0}^2 \sum_{m=-l}^l C_{lm}^i P_l(\mathbf{r}) Y_l^m(\hat{\Omega}_{\mathbf{r}}).$$

Taking matrix elements of the many-electron Hamiltonian

$$\langle \Phi_i | H | \Phi_j \rangle = 1N_L^{-1} \sum_{\mathbf{R}} \sum_{\mathbf{R}'} \sum_{l=0}^2 \sum_{l'=0}^2 \sum_{m=-l}^l \sum_{m'=-l'}^{l'} C_{lm}^{i*} C_{l'm'}^j \exp[i(\mathbf{k}_j \cdot \mathbf{R}' - \mathbf{k}_i \cdot \mathbf{R})] \epsilon_{ll'mm'}(\mathbf{R}, \mathbf{R}'),$$

where

$$\epsilon_{ll'mm'}(\mathbf{R}, \mathbf{R}') = \int d\mathbf{r} P_l^*(|\mathbf{r}-\mathbf{R}|) Y_l^{m*}(\hat{\Omega}_{\mathbf{r}-\mathbf{R}}) H P_{l'}(|\mathbf{r}-\mathbf{R}'|) Y_{l'}^{m'}(\hat{\Omega}_{\mathbf{r}-\mathbf{R}'}).$$

Since the Hamiltonian is the same at all lattice sites, this matrix element can be written as

$$\langle \Phi_i | H | \Phi_j \rangle = \delta_{k_i, k_j} \sum_{l=0}^2 \sum_{l'=0}^2 \sum_{m=-l}^l \sum_{m'=-l'}^{l'} C_{lm}^{i*} C_{l'm'}^j \mu_{ll'mm'}(\mathbf{k}_i),$$

where

$$\mu_{ll'mm'}(\mathbf{k}) = \sum_{\mathbf{R}} \exp(i\mathbf{k} \cdot \mathbf{R}) \epsilon_{ll'mm'}(\mathbf{R}).$$

The coefficients and energies are determined by diagonalizing the $\mu_{ll'mm'}$ matrix, solving the resulting matrix (which is 9×9 for $l_{\max}=2$) along the symmetry axes (where the matrix can be subdivided into 4×4 or less matrices) exactly as a function of the $\epsilon_{ll'mm'}(\mathbf{R})$, and fitting these functions to the published band structures. The fits were made using 33 $\epsilon_{ll'mm'}(\mathbf{R})$ as independent parameters corresponding to third nearest neighbors—resulting in a root-mean-square error of less than 0.006H (1 H = 27.2 eV) for all necessary bands (compared to a Fermi energy of order 0.1 H).

The radial wave functions are calculated separately using an atomic Hartree-Fock method. The wave functions calculated in this way are only approximate though. For each excitation a Hartree-Fock calculation is done with one de-occupied ground-state orbital and one occupied excited orbital (of a different symmetry). Thus to obtain the radial wave functions used in the $2P \rightarrow 3S$ transition in sodium, a Hartree-Fock calculation was performed using three fully occupied S orbitals and one $\frac{5}{6}$ th occupied p orbital. The basis sets for the calculation were of the Slater type taken from Ref. 15 (with a few extra valence Slater orbitals added). The electron-electron integrals using these wave functions are generally within 30% of integrals obtained using results of free-electron models¹⁸ and cluster models.⁷

The above procedure assumes that the symmetries (s , p , or d) of the hole and excited electron and their energy difference can be accurately obtained from the ground-state calculation but the radial orbitals are obtained from

an excited (but atomic) state calculation. This allows for the contraction of the orbitals at the site of the hole. One could, of course, have included many more virtual ground-state bands in the basis set—obtaining the necessary variational freedom, but this would make the problem computationally impossible. The above approximation, of using ground-state-theory energy differences, ignores a number of correlation effects, including the following: (1) The on-site energy interaction integrals have different screening corrections in the ground state than in the excited states and (2) the excited atom has smaller near-neighbor interaction integrals.

C. Monte Carlo calculation of interaction

To determine the approximations for the wave functions (the Ψ^I and Ψ^F), a finite set of Slater determinates (the ψ_A) is chosen and the matrix $\langle \psi^A | H | \psi^B \rangle$ is diagonalized. It is assumed that the ground-state wave function (Ψ^I) can be satisfactorily represented by the self-consistent one-electron state. But the excited states (Ψ^F) cannot necessarily be represented by only one electron-hole state ($|u, v\rangle = a_u^\dagger a_v |\Psi^I\rangle$) since these states are not self-consistent. Therefore, the chosen set will contain the ground state and as large a randomly chosen set of the $|u, v\rangle$ as possible. (Other states with more than one electron-hole pair come into the calculation at higher order and are not considered here.) The Hamiltonian matrix element between these states is

$$\langle u', v' | H | u, v \rangle = V_{u', v', v', u} - V_{u', v, u, v'},$$

where $V_{u', v', v', u}$ is the screened Coulomb matrix element between the independent-electron states $\Phi_{u'}$ and Φ_v and $\Phi_{v'}$ and Φ_u :

$$V_{u',v,v',u} = \int d\mathbf{r} \int d\mathbf{r}' \Phi_{u'}^*(\mathbf{r}) \Phi_v^*(\mathbf{r}') \exp(-k_0|\mathbf{r}-\mathbf{r}'|)/|\mathbf{r}-\mathbf{r}'| \Phi_{v'}(\mathbf{r}) \Phi_u(\mathbf{r}').$$

(A sum over spin indices is included in the integrals.)

The $|u,v\rangle$ are sampled by first randomly choosing a k from the first Brillouin zone (u and v must have the same k for optical absorption) and then randomly choosing a ground-state band less than the Fermi energy, e_F , for Φ_u and an excited-state band greater than e_F for Φ_v . The eigenvectors of this many-electron Hamiltonian matrix between the randomly chosen $|u,v\rangle$ will be the approximations for the Ψ^F , the excited states.⁸

The $|u,v\rangle$ are not chosen by a grid scheme since a physical grid would either artificially have too many degenerate states with too large of gaps (in energy) between, or else the grid would have an artificial lack of degeneracies. Randomly choosing the $|u,v\rangle$ does not ensure the proper density of states, but it will ensure a proper mixture of nearly degenerate to not degenerate states (over a large random sample). Any sampling method that properly represents the density of states should give similar results.

For optical absorption, u and v must have the same spin; matrix elements between states with the spin of u' and v' the same as the spin of u and v are between three and eight times as large as matrix elements between states with the spin of u' and v' different from the spin of u and

v . ($V_{u',v,v',u}$ is much smaller than $V_{u',v,u,v'}$.) Thus spin states almost decouple, and therefore one can do the calculation fairly accurately by considering only one spin state. This is not ideal, but the additional matrix size makes considering both sets of spin states a costly endeavor (mainly because it would require a computer larger than the 2-megaword FPS164 array processor on which the codes were written).

Note that all of the nondiagonal matrix elements are of order $1/N_L$, so that there is little mixing between these states unless the states are sufficiently dense. If there is significant density, the states will couple and the correlation can be quite large—possibly forming an excitonic threshold singularity. Within the randomly chosen submatrix, the average spacing between states is increased by the ratio of N_L to the submatrix order M . Thus the $V_{u,v,v',u}$ must be scaled by the same ratio to obtain the correct mixing among the chosen states.

D. Calculation of absorption coefficients

Now that the wave functions and energies have been calculated for the Ψ^F , Fermi's golden rule can be used to calculate the unpolarized optical absorption rate and oth-

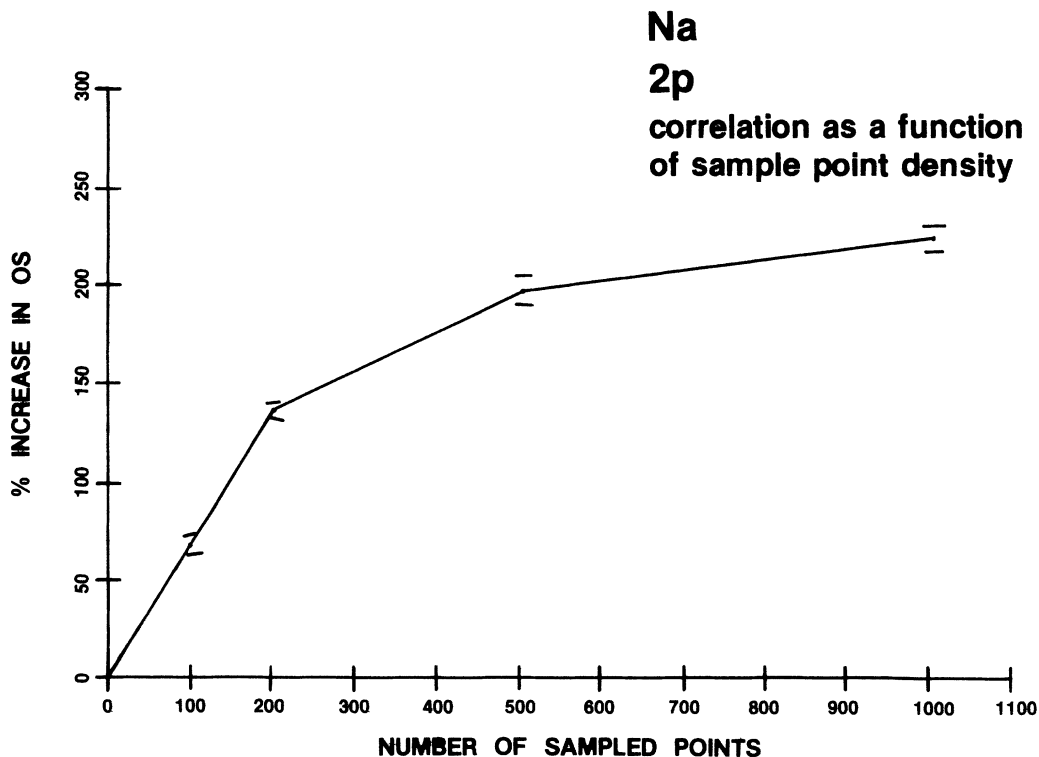


FIG. 2. The percent increase in the height of the threshold peak in the correlated oscillator strength (over the height of the threshold peak in the uncorrelated oscillator strength) for the 2p-3s transition in sodium as the number of points in each Monte Carlo sample is increased. (1018 is the maximum number allowed by an FPS164.)

er optical properties,⁴

$$W_{FI} = (4\pi^2 n_\gamma / 3) / E_\gamma |\nabla_{FI}|^2 \gamma (E_F - E_I - E_\gamma),$$

where

$$\nabla_{FI} = \sum_{i,j} \nabla_{ij} \langle \Psi^F | a_i^\dagger a_j | \Psi^I \rangle,$$

$$\nabla_{ij} = \int d\mathbf{r} \Phi_i^*(\mathbf{r}) \nabla \Phi_j(\mathbf{r}).$$

To get the total optical absorption rate at E , a sum over the possible excited states (the Ψ^F) is completed. And since the number of states times the average of some function of the states yields the sum of the function of the states, one can obtain

$$W(E_\gamma) = (4\pi^2 n_\gamma / 3) / E_\gamma \langle |\nabla_{FI}|^2 \rangle D_J(E_\gamma),$$

where $\langle |\nabla_{FI}|^2 \rangle$ is the average of all the $|\nabla_{FI}|^2$ with the same energy difference $E_F - E_I = E_\gamma$ and $D_J(E_\gamma)$ is the joint density of states at energy E_γ .

Most absorption functions are written in terms of a unitless function, the oscillator strength $f_{FI} = (\frac{2}{3}) / E_\gamma |\nabla_{FI}|^2$ or $\langle f_{FI} \rangle (2/3) / E_\gamma \langle |\nabla_{FI}|^2 \rangle$,

$$W = 2\pi^2 n_\gamma \langle f_{FI} \rangle g_J(E_\gamma) = \text{absorption rate}$$

and

$$\mu = 2\pi^2 \alpha \langle f_{FI} \rangle g_J(E_\gamma) = \text{absorption coefficient},$$

where $g_J(E_\gamma)$ is the joint density of states per unit volume and α is the fine-structure constant.

III. RESULTS

Figure 2 shows the percent increase in absorption at the $2p$ - $3s$ transition in sodium as a function of the number of points sampled. The maximum number of points that can fit in memory on our FPS164 is 1018, which is just about at the point where the curve is leveling off.

The correlated and uncorrelated oscillator strengths for this same transition in sodium are shown in Fig. 3. A more general use of the term "correlated" is used here. By the term "correlated," the authors mean any many-body correction (besides screening) to the result of the Hartree-Fock bands (which include screening). Clearly there is quite a large amount of correlation at the threshold peak; this is indicative of a strong electron-hole coupling (implying excitonic structure). The $2p$ - $4s$ and $3p$ - $4s$ transitions in potassium show similar increases between the correlated and uncorrelated oscillator strengths.

Figures 4-7 show comparisons between experimental spectra and the corresponding theoretical results for various excitations in the metallic systems used. In all four graphs the horizontal position (the threshold energy) of the theoretical curve and the vertical scale of the experimental curve were arbitrary and were set to maximize similarities at the threshold peaks. For the $2p$ - $3s$ transi-

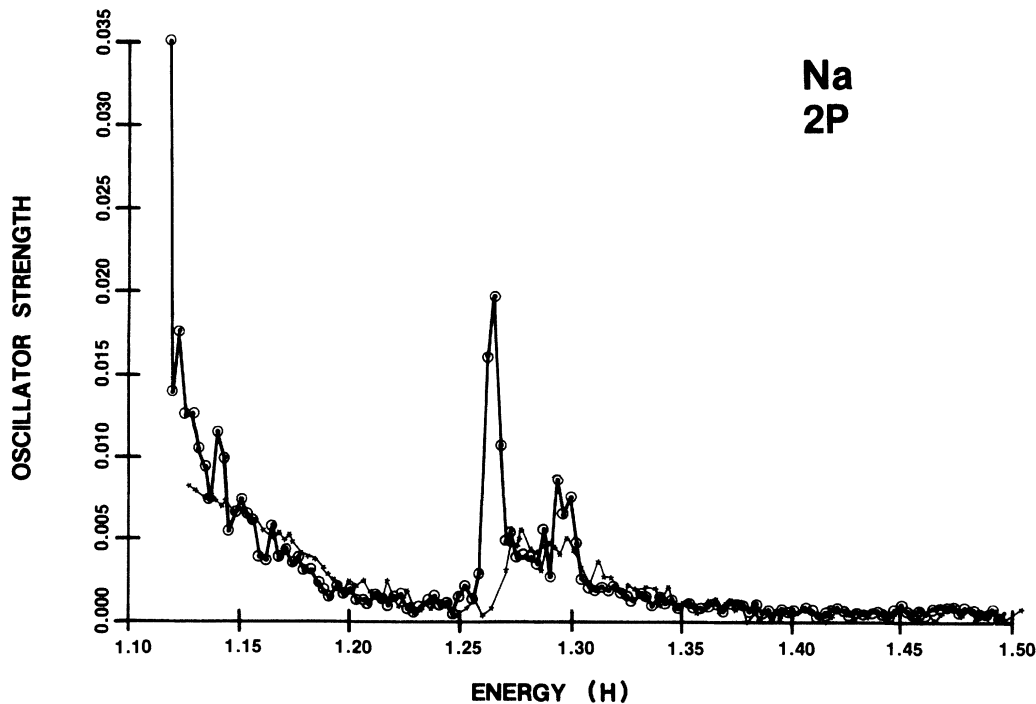


FIG. 3. The oscillator strength (averaged over three runs) of both the correlated line and the uncorrelated line (which includes screening but not any other many-body effects) results for the $2p$ - $3s$ transition in sodium. The uncorrelated curve comes direct from the band structure. The correlated curve includes the results of the diagonalization of the (screened) Hamiltonian for the three randomly chosen sets of states. The large increase after the diagonalization of the threshold edge is indicative of an excitonic threshold peak. Note also that significant differences (besides the fluctuations due to the randomly chosen sets) between the two curves occur only near the threshold.

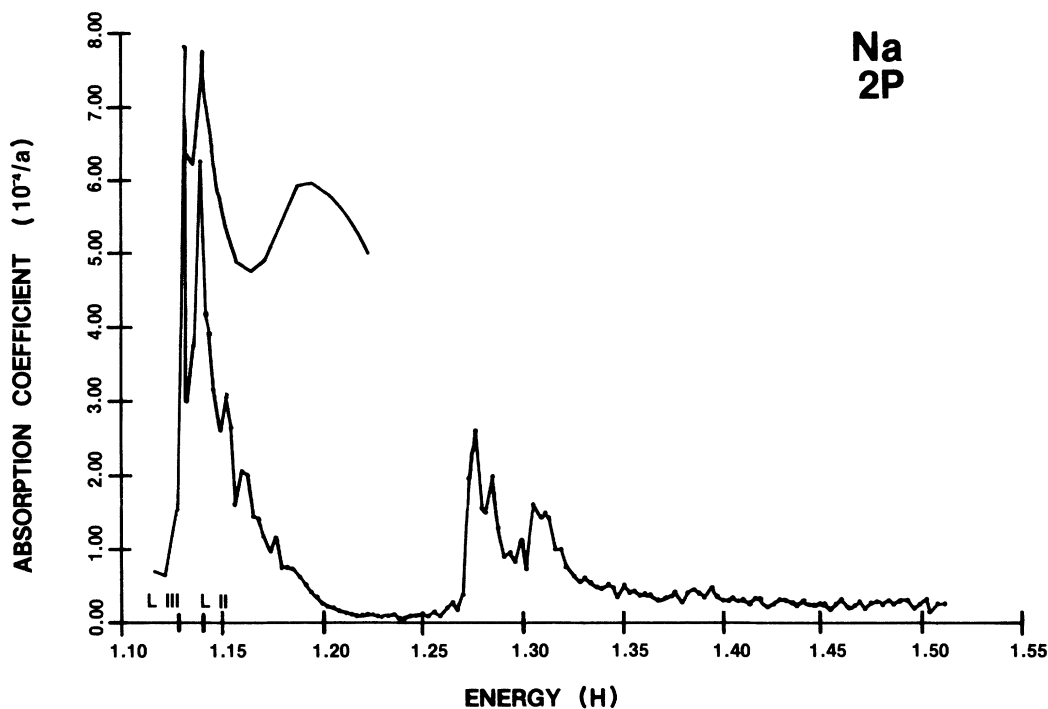


FIG. 4. The correlated absorption spectrum of the $2p$ - $3s$ transition in sodium metal (for the same three runs used in Fig. 3 and the experimental spectrum by Haensel *et al.* (Ref. 20). Both experiment and theory exhibit threshold excitons. The two peaks are spin-orbit partners; these are incorporated into the calculation by taking the single-spin results, shifting according to the experimental results, multiplying by the spin degeneracy, and adding the two spin partners together.

tion in sodium and the $3p$ - $4s$ transition in potassium, the two spin-orbit peaks were calculated separately, were given different threshold energies, and then were added together.

Note that the calculated results have many more fluctuations; these are due to the incorporation of Monte Carlo methods and most can be smoothed out by making more runs (each theoretical curve shown is the average of

three runs of 1000 points each). Time and finances were the limiting considerations in the number of runs done. But we were most interested in establishing the existence (or nonexistence) of the threshold peaks; thus fluctuations (which are small compared to peak size) are of minor concern.

Also, the large amount of dissimilarity between experiment and theory away from the threshold peak is mainly

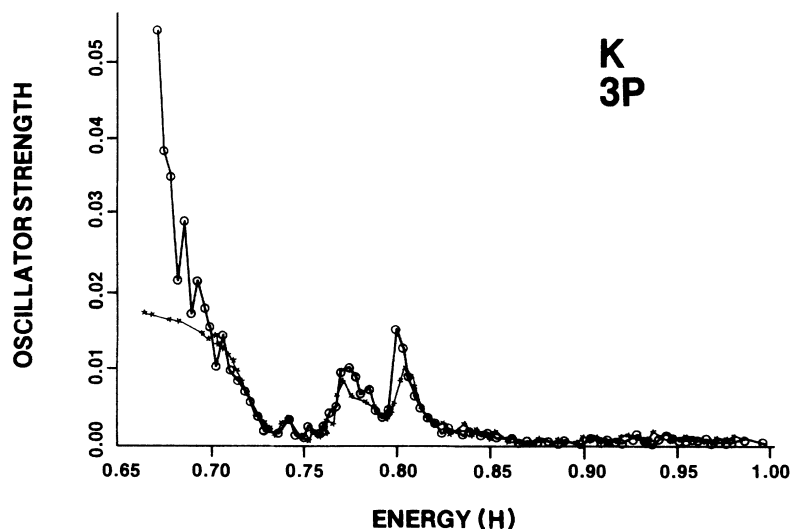


FIG. 5. The correlated (*) and uncorrelated (○) oscillator strengths for the $3p$ - $4s$ transition in potassium.

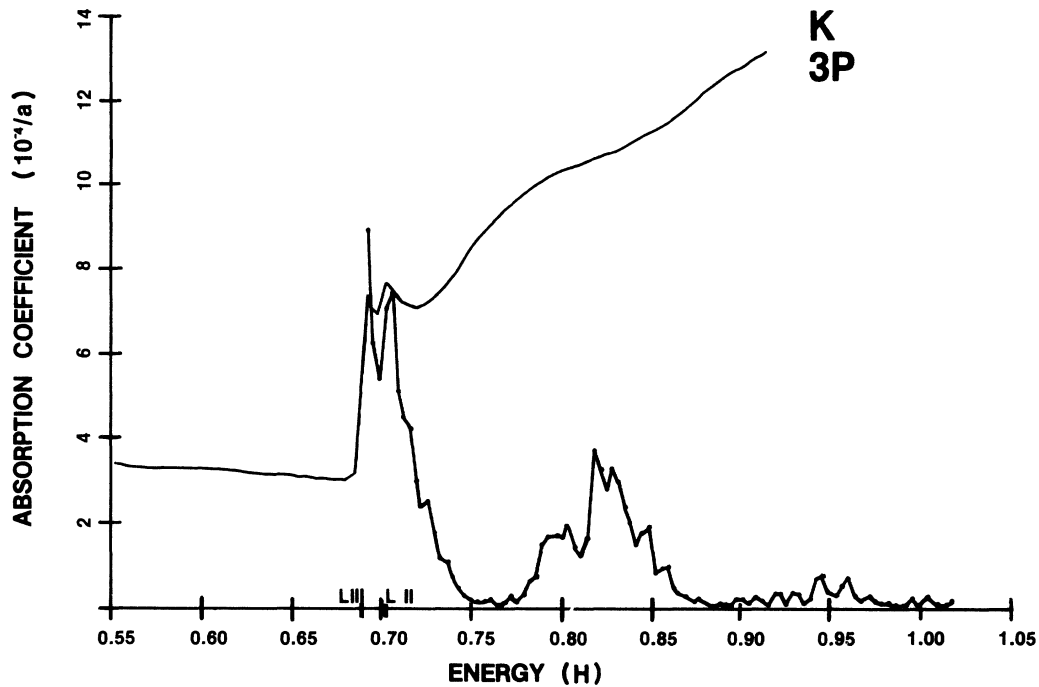


FIG. 6. The correlated absorption spectrum of the $3p$ - $4s$ transition in potassium metal and the experimental spectrum by Ishii *et al.* Both experiment and theory exhibit threshold excitons. The two peaks are spin-orbit partners.

due to the local-density methods used to calculate the band structures to which we fit our simplified LCAO bands and to the approximations involved in the fit, but are not due to the method we used to calculate the correlation between the bands. This is shown clearly in Fig. 3; the difference that the Monte Carlo diagonalization caused is only significant at the edge. Local-density methods are only accurate near the Fermi energy, up to

where the threshold states are excited. Thus the method can still be considered accurate at the threshold, but not away from it.

Also, the method does not take phonon broadening of the peaks into account. Notice that the heights of the peaks of the theoretical curves for the two different spin-orbit partners are reversed in the experimental curves. If phonon broadening could be included in the theoretical

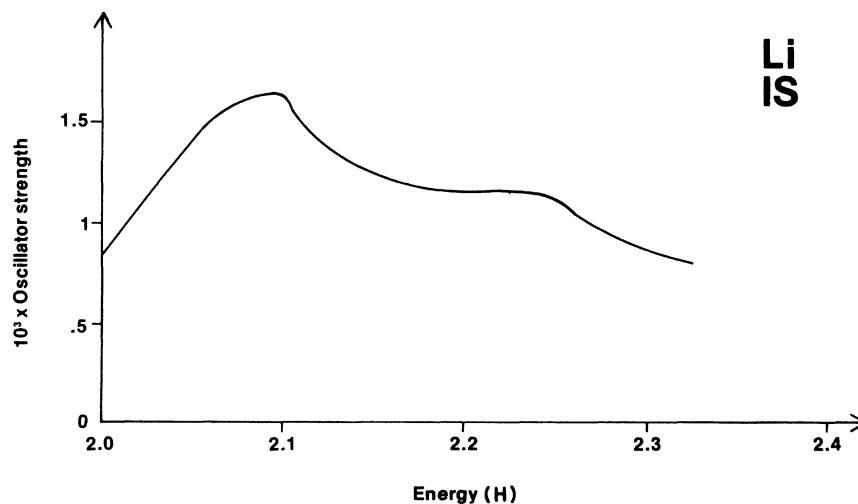


FIG. 7. The oscillator strength for the $1s$ - $2p$ transition in lithium. The calculated correlated and uncorrelated spectra differ by less than 3×10^{-5} .

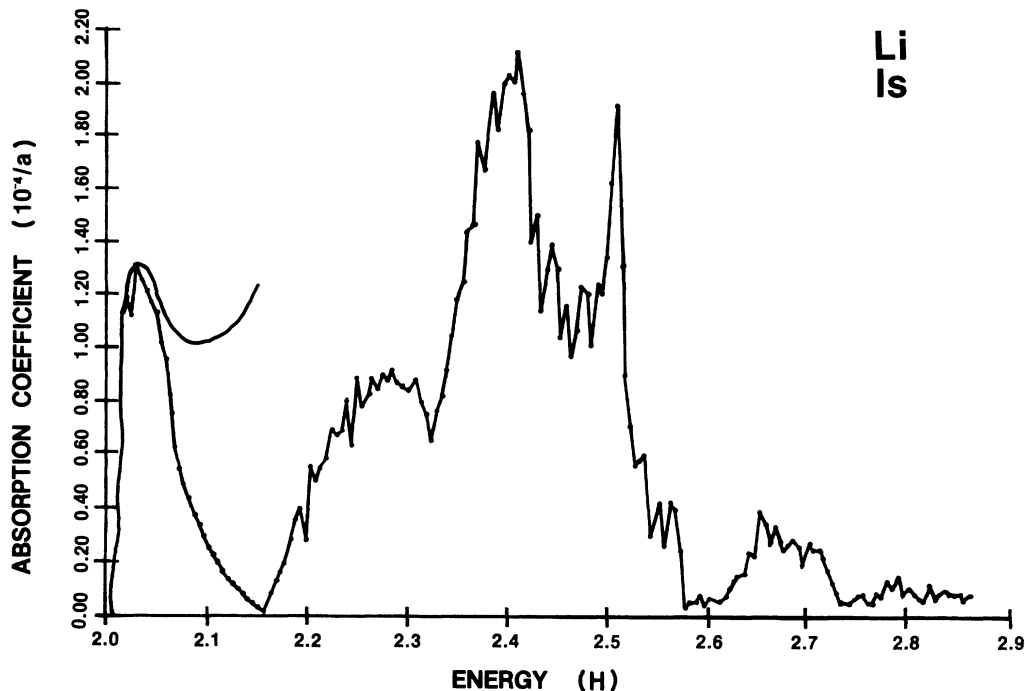


FIG. 8. The correlated absorption spectrum of the $1s-2p$ transition in lithium metal and the experimental spectrum by Myers and Sixtensson (Ref. 28). Neither experiment nor theory shows excitonic effects.

model, the overlap between the two spin-orbit partners would be considerably larger, thus changing the relative heights of the two peaks.

IV. CONCLUSIONS

Generally, the theoretical model presented in this paper is consistent with known experimental results, in that

excitonic threshold peaks were found for all transitions that are experimentally known to have threshold peaks. The results for the total absorption spectra may not reflect the experiment to much accuracy, but the model is mainly concerned only with the spectra at threshold and performs acceptably well there.

In order to get a nearly localized state out of delocal-

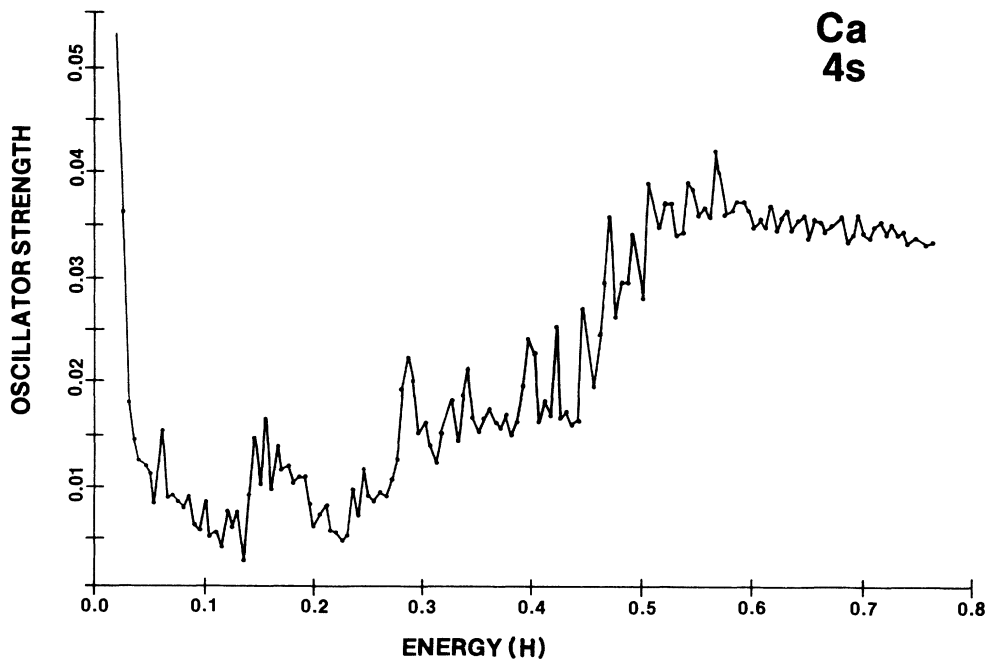


FIG. 9. The oscillator strength for the $4s-4p$ transition in calcium. The calculated correlated and uncorrelated spectra differ by less than 0.002.

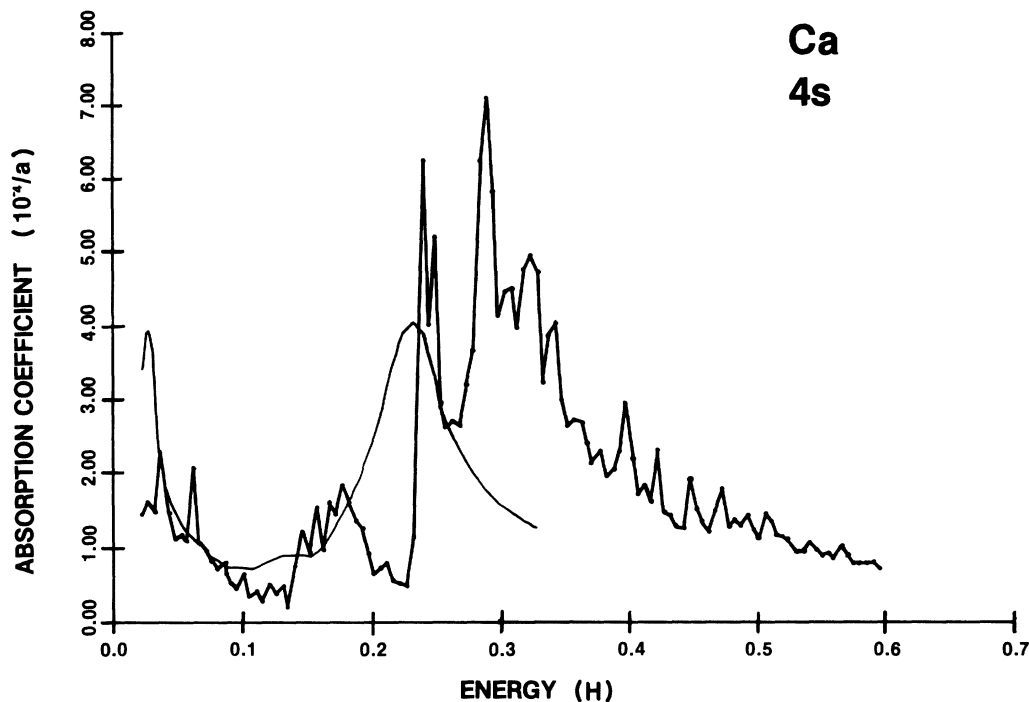


FIG. 10. The correlated absorption spectrum of the $4s$ - $4p$ transition in calcium metal and the experimental spectrum by Hunderi (Ref. 24). The experimental curve shows the possibility of an excitonic peak, but the theory shows none.

ized orbitals, the wave functions must contain a significant number of the orbitals. This combination of a large number of orbitals greatly increases the oscillator strength

$$f_{FI} = (2/3)/E_{\gamma} \left| \sum_{i,j} \langle \Psi^f | a_i^{\dagger} a_j | \Psi^I \rangle \nabla_{ij} \right|^2,$$

since the term within the $||$ is approximately (since ∇_{ij} does not vary much) just a sum of the eigenvector components (each represents one delocalized electron-hole pair orbital) of the final-state wave function. (Ψ^I , the initial state, contains no excited electrons and no holes.) Thus, a large mixing between orbitals will increase the oscillator strength—possibly making a threshold peak.

The main condition for large mixing is a high ratio of the average interaction potential (between the electron-hole pairs) to the average spacing between states near threshold. Or, equivalently, a high value of the average

interaction potential (which scales as $1/N$) times the density of states (which scales as N) is needed.

The calcium $4s$ - $4p$ transition (Figs. 8–10) compares least well with the experimental threshold shape. The experimentalists did not continue to low enough energy to obtain information on the Drude section of the spectra. The experiment appears to exhibit an excitonic peak, but without knowledge of the Drude part of the curve, it is uncertain whether or not the interband absorption spectrum alone exhibits a threshold singularity. The theoretical model implies no singularity, but experimentally the interband absorption spectrum is uncertain.

ACKNOWLEDGMENTS

This work was supported by the National Science Foundation under a National Science Foundation Graduate Fellowship and under Grant No. DMR 80-20520.

*Present address: Department of Physics, Morningside College, Sioux City, IA 51106.

¹N. W. Ashcroft and N. D. Mermin, *Solid State Physics* (Saunders College, New York, 1976).

²D. J. Stevenson, *Phys. Rev. B* **7**, 2348 (1973).

³W. Y. Ching and J. Callaway, *Phys. Rev. B* **9**, 5115 (1974).

⁴W. B. Fowler, *Physics of Color Centers* (Academic, New York, 1968).

⁵M. H. Cohen, *Optical Properties and Electronic Structure of Metals and Alloys* (North-Holland, Amsterdam, 1966).

⁶J. C. Boisvert, P. W. Goalwin, A. B. Kunz, M. H. Bakshi, and

C. P. Flynn, *Phys. Rev. B* **31**, 4984 (1985).

⁷C. Woodward, thesis, University of Illinois, 1985.

⁸G. D. Mahan, in *Solid State Physics* (Academic, New York, 1974), Vol. 29.

⁹P. Nozières and C. T. De Dominicis, *Phys. Rev.* **178**, 1097 (1969).

¹⁰G. D. Mahan, *Phys. Rev. B* **11**, 4814 (1975).

¹¹J. D. Dow, *Phys. Rev. B* **9**, 4165 (1974).

¹²J. D. Dow, D. L. Smith, and B. F. Sonntag, *Phys. Rev. B* **10**, 3092 (1974).

¹³J. D. Dow, D. L. Smith, D. R. Franceschetti, J. E. Robinson,

- and T. R. Carver, Phys. Rev. B **16**, 4707 (1977).
- ¹⁴U. von Barth and G. Grossmann, Phys. Rev. B **25**, 5150 (1982).
- ¹⁵E. Clementi and C. Roetti, At. Data Nucl. Phys. Tables **14**, 177 (1974).
- ¹⁶O. Gunnarsson and K. Schonhämmer, Phys. Rev. B **26**, 2765 (1982).
- ¹⁷B. W. Veal and A. P. Paulikas, Phys. Rev. B **31**, 5399 (1985).
- ¹⁸C. P. Flynn and A. B. Kunz, Int. J. Quantum Chem. Symp. **17**, 573 (1983).
- ¹⁹A. B. Kunz and C. P. Flynn, Phys. Rev. Lett. **50**, 1524 (1983).
- ²⁰R. Haensel, G. Keitel, P. Schreiber, and B. Sonntag, Phys. Rev. Lett. **23**, 528 (1969).
- ²¹T. Ishii, Y. Sakisaka, and S. Yamagushi, J. Phys. Soc. Jpn. **42**, 876 (1977).
- ²²A. G. Mathewson and H. P. Myers, J. Phys. F **3**, 623 (1973).
- ²³C. Kunz, R. Haensel, G. Keitel, P. Schreiber, and B. Sonntag, *Electron Density of States*, Natl. Bur. Stand. (U.S.) Circ. No. 323 (U.S. GPO, Washington, D. C., 1971).
- ²⁴O. Hunderi, J. Phys. F **6**, 1223 (1976).
- ²⁵H. A. Bethe and R. Jackiw, *Intermediate Quantum Mechanics*, 2nd ed. (Benjamin, Holland, 1968).
- ²⁶J. C. Slater and G. F. Koster, Phys. Rev. **94**, 1498 (1954).
- ²⁷Lithium: W. Y. Ching and J. Callaway, Phys. Rev. B **9**, 5115 (1974); sodium: W. Y. Ching and J. Callaway, *ibid.* **11**, 1324 (1975); potassium: W. Y. Ching and J. Callaway, Phys. Rev. Lett. **30**, 441 (1973); calcium: D. J. Mickish, A. B. Kinz and S. T. Patelides, Phys. Rev. B **10**, 1369 (1974); aluminum: V. Hofstein and D. S. Boudreaux, *ibid.* 3013 (1970).
- ²⁸H. P. Myers and P. Sixtensson, J. Phys. F **6**, 2023 (1976).